

Next-to-leading order QCD calculation of B_c to charmonium tensor form factors

Wei Tao^{*,1}, Zhen-Jun Xiao^{†,1} and Ruilin Zhu^{‡1}

¹ *Department of Physics and Institute of Theoretical Physics,
Nanjing Normal University, Nanjing, Jiangsu 210023, China*

(Dated: June 8, 2022)

We present a next-to-leading order (NLO) QCD corrections to $B_c \rightarrow \eta_c$ and $B_c \rightarrow J/\psi$ tensor form factors within nonrelativistic QCD (NRQCD) framework. The full analytical results for B_c to S-wave charmonium tensor form factors are obtained. We also studied the asymptotic behaviours of tensor form factors in hierarchy heavy quark limit, i.e. $m_b \rightarrow \infty$, $m_c \rightarrow \infty$, and $m_c/m_b \rightarrow 0$. A compact expression for tensor form factors are given analytically in the hierarchy heavy quark limit. The relation among different form factors is also analyzed especially at large momentum recoil point. The numerical results for the B_c to charmonium tensor form factors in all the physical region are given in the end.

PACS numbers 12.38.Bx, 13.25.Gv, 14.40.Pq

I. INTRODUCTION

Testing the Standard Model and hunting for new physics is a primary task in particle physics. In recent years, the $b \rightarrow c$ transition has been employed as a vivid window to indirectly detect the possible pattern of new physics. Particularly the $R(D^{(*)})$ and $R(J/\psi)$ anomalies in recent flavor physics experiments shall challenge the lepton universality and indicate the possible pattern of new physics [1–4]. To distinguish new physics signal from background in these heavy flavor quark decay channels, a precision calculation and analysis of transition form factors is required [5–8].

The $b \rightarrow c$ transition modes in the B_c meson has been studied in lots of frameworks: the lattice QCD simulations [9, 10], the nonrelativistic QCD(NRQCD) approach [11–18], the perturbative QCD approach [19–23], the principle of maximum conformality [24], the QCD sum rules [25–27], the light-cone sum rules [28], the light-front quark model [29, 30], the relativistic quark model [31–35], the nonrelativistic constituent quark model [36] and the SU(3) symmetry [37, 38]. It is a remarkable progress that the HPQCD collaboration have gained the first lattice QCD results for the $B_c \rightarrow J/\psi$ vector and axial-vector form factors in the full q^2 range [10]. Using the lattice QCD computation of the $B_c \rightarrow J/\psi$ form factors, the HPQCD collaboration then determine the standard model predictions of $R(J/\psi)$ and improve the theoretical precision. Therein the lattice QCD results have reduced the tension of $R(J/\psi)$ anomalies and also indicated the LHCb data has a 1.8σ deviation from the standard model prediction. To include the possible new physics, other form factors such as scalar, pseudoscalar, and tensor form factors are also involved in the processes, apart from vector and axial-vector form factors. These new form factors are not simulated in lattice QCD currently. Fortunately, one can perturbatively calculate these form fac-

tors at large momentum recoil order by order in NRQCD approach.

NRQCD is a powerful theoretical framework to deal with the production and decay of double heavy quark system [39]. There are three kinds of typical scales ordered by the quark relative velocity v : the heavy quark mass (m_Q), around and above which the perturbative interactions dominate for the hadron production and decay; the heavy quark relative momentum ($m_Q v$); the heavy quark kinetic energy ($m_Q v^2$), around which the nonperturbative binding dominate. The form factors can be expressed by the series of nonperturbative long-distance matrix elements (LDMEs) and the corresponding perturbative Wilson coefficients. In this paper, we major focus on the next-to-leading order (NLO) QCD corrections to the $B_c \rightarrow \eta_c$ and $B_c \rightarrow J/\psi$ form factors. The scalar and pseudoscalar form factors can be obtained from vector and axial-vector form factors by equation of motion. Thus we will calculate the $B_c \rightarrow \eta_c$ and $B_c \rightarrow J/\psi$ tensor form factors at NLO in NRQCD framework.

Even though the definition of form factors only relies on the local bilinear current, there needs a new renormalization factor to cancel the UV divergence since the tensor current is not a conserved current. We will check the UV and IR behaviour of the $B_c \rightarrow \eta_c$ and $B_c \rightarrow J/\psi$ tensor form factors. On the other hand, we will investigate the relation among different form factors in the hierarchy heavy quark limit. Previous studies have indicate that there are degenerate for vector and axial-vector form factors in hierarchy heavy quark limit. Very similarly to Isgur-Wise function in small momentum recoil, the form factors are not independent at large momentum recoil. Thus we will check the asymptotic expressions of tensor form factors in the hierarchy heavy quark limit.

The paper is arranged as follows. We give the definition and the LO results for $B_c \rightarrow \eta_c$ and $B_c \rightarrow J/\psi$ tensor form factors in Section II. We present the NLO QCD corrections to the $B_c \rightarrow \eta_c$ and $B_c \rightarrow J/\psi$ tensor form factors, discuss the UV and IR behaviours, and give the asymptotic analysis of tensor form factors in the hierarchy heavy quark limit in Section III. Numerical results and discussions are given in Section IV. In the end we give the conclusion.

*taowei@njnu.edu.cn

†Corresponding author: xiaozhenjun@njnu.edu.cn

‡Corresponding author: rllzhu@njnu.edu.cn

II. $B_c \rightarrow \eta_c$ AND $B_c \rightarrow J/\psi$ TENSOR FORM FACTORS

Inputting various Dirac Gamma matrixes in bilinear local quark current sandwiched between the B_c meson and a charmonium states, one can define various form factors. The tensor form factors for B_c meson into a S-wave charmonium are defined as [40–43]

$$\langle \eta_c(p) | \bar{c} \sigma^{\mu\nu} q_\nu b | B_c(P) \rangle = \frac{f_T(q^2)}{m_{B_c} + m_{\eta_c}} \left(q^2 (P^\mu + p^\mu) - (m_{B_c}^2 - m_{\eta_c}^2) q^\mu \right), \quad (1)$$

$$\langle J/\psi(p, \varepsilon^*) | \bar{c} \sigma^{\mu\nu} q_\nu b | B_c(P) \rangle = 2iT_1(q^2) \epsilon^{\mu\nu\rho\sigma} \varepsilon_\nu^* p_\rho P_\sigma, \quad (2)$$

$$\begin{aligned} \langle J/\psi(p, \varepsilon^*) | \bar{c} \sigma^{\mu\nu} \gamma^5 q_\nu b | B_c(P) \rangle \\ = T_2(q^2) \left((m_{B_c}^2 - m_{J/\psi}^2) \varepsilon^{*\mu} - \varepsilon^* \cdot q (P^\mu + p^\mu) \right) \\ + T_3(q^2) \varepsilon^* \cdot q \left(q^\mu - \frac{q^2}{m_{B_c}^2 - m_{J/\psi}^2} (P^\mu + p^\mu) \right), \end{aligned} \quad (3)$$

where Dirac operator $\sigma^{\mu\nu} = \frac{i}{2}(\gamma^\mu \gamma^\nu - \gamma^\nu \gamma^\mu)$. We denote the momentum transfer as $q = P - p$ and we have the physical constraint $0 \leq q^2 \leq (m_{B_c} - m_{J/\psi(\eta_c)})^2$ in form factors. The m

and ε are the mass and polarization vector of the mesons. We also use the convention of Levi-Civita tensor $\epsilon^{0123} = 1$. Note that $T_1(0) = T_2(0)$ by using the identities $\sigma_{\mu\nu} \gamma_5 = \frac{i}{2} \epsilon_{\mu\nu\rho\sigma} \sigma^{\rho\sigma}$ and $\epsilon_{\mu\nu\rho\sigma} \sigma^{\mu\nu} \gamma_5 = -2i \sigma_{\rho\sigma}$ in Eqs. (2) and (3).



FIG. 1: Tree level diagrams for the form factors of B_c into a S-wave charmonium, where the symbol “ \oplus ” denotes certain current operators and the lower line is the spectator charm quark. At LO, one gluon is exchanged between the upper bottom/charm quark and the lower charm quark.

In NRQCD, both the B_c meson and J/ψ can be treated as nonrelativistic bound states. The decay amplitudes for $B_c \rightarrow J/\psi$ can be factorized as the short-distance Wilson coefficients and the LDMEs [11, 16, 39, 44]. The LO Feynman diagrams are plotted in Fig. 1. Using NRQCD, the leading order results for the form factors are

$$f_T^{\text{LO}}(z, s) = \frac{16 \sqrt{2} C_A C_F \pi s^2 (z+1)^{3/2} (3z+1) \alpha_s \psi(0)_{B_c} \psi(0)_{\eta_c}}{z^{3/2} (sz^2 - 2sz + 1)^2 m_b^3 N_c}, \quad (4)$$

$$T_1^{\text{LO}}(z, s) = \frac{4 \sqrt{2} C_A C_F \pi s \sqrt{z+1} (5sz^2 + 6sz + 4s + 1) \alpha_s \psi(0)_{B_c} \psi(0)_{J/\psi}}{z^{3/2} (sz^2 - 2sz + 1)^2 m_b^3 N_c}, \quad (5)$$

$$T_2^{\text{LO}}(z, s) = \frac{4 \sqrt{2} C_A C_F \pi \sqrt{z+1} (15s^2 z^4 + 8s^2 z^3 - 8s^2 z^2 - 16s^2 z + 6s^2 z^2 - 4s - 1) \alpha_s \psi(0)_{B_c} \psi(0)_{J/\psi}}{(z-1) z^{3/2} (3z+1) (sz^2 - 2sz + 1)^2 m_b^3 N_c}, \quad (6)$$

$$T_3^{\text{LO}}(z, s) = -\frac{4 \sqrt{2} C_A C_F \pi s \sqrt{z+1} (3sz^2 + 2sz - 4s - 1) \alpha_s \psi(0)_{B_c} \psi(0)_{J/\psi}}{z^{3/2} (sz^2 - 2sz + 1)^2 m_b^3 N_c}, \quad (7)$$

where $z = m_c/m_b$ and $s = 1/(1 - q^2/m_b^2)$. The nonperturbative parameters $\psi(0)_{B_c}$ and $\psi(0)_{J/\psi(\eta_c)}$ are the Schrödinger wave functions at the origin for $b\bar{c}$ and $c\bar{c}$ systems, respectively, which are related to the NRQCD LDMEs for the production and decay processes [39].

It is noted that the heavy quark symmetry is involved at leading power in heavy quark effective theory and the form factors at minimum momentum recoil point can be expressed by the Isgur-Wise functions. It indicates that the heavy-to-heavy transition form factors are not independent in heavy quark symmetry. In this paper, we will calculate perturbatively the form factors of B_c into a S-wave charmonium. The perturbative calculation results are thought to be solid at the maximum momentum recoil region. Then we can also investigate the asymptotic behaviors in hierarchy heavy quark limit. We introduce the hierarchy heavy quark limit, i.e. $m_b \rightarrow$

∞ , $m_c \rightarrow \infty$, and $z = m_c/m_b \rightarrow 0$ to observe the asymptotic behaviors. One can assume the heavy quark mass approaching the infinity as $m_c = x^a|_{x \rightarrow \infty, a>0}$ and $m_b = x^b|_{x \rightarrow \infty, a>0}$, and then $z = m_c/m_b = x^{a-b}|_{x \rightarrow \infty, a<b} \rightarrow 0$. One can easily see that the form factors are not independent in this limit. In the following we list the asymptotic expression for the LO tensor form factors

$$f_T^{\text{Asymp. LO}}(z, s) = \frac{16 \sqrt{2} C_A C_F \pi s^2 \alpha_s \psi(0)_{B_c} \psi(0)_{\eta_c}}{z^{3/2} m_b^3 N_c}, \quad (8)$$

$$T_1^{\text{Asymp. LO}}(z, s) = \frac{4 \sqrt{2} C_A C_F \pi s (4s+1) \alpha_s \psi(0)_{B_c} \psi(0)_{J/\psi}}{z^{3/2} m_b^3 N_c}. \quad (9)$$

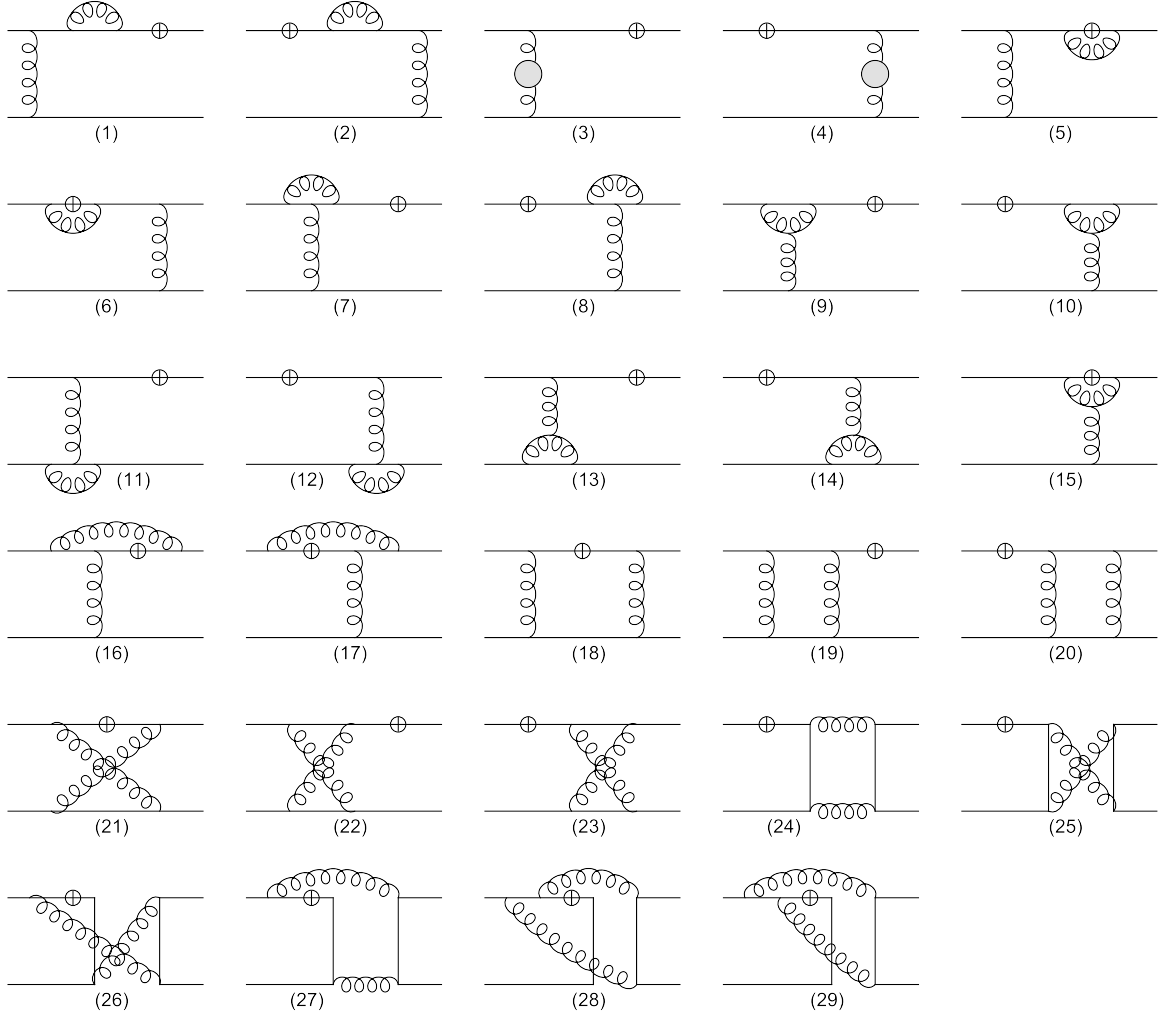


FIG. 2: All of 1-loop diagrams for the form factors of $B_c \rightarrow J/\psi(\eta_c)$, where the symbol “ \oplus ” denotes certain current operators. The bubble in the sub-diagrams (3-4) represents the 1-loop gluon self-energies. The sub-diagrams (24-29) only contribute to $B_c \rightarrow \eta_c$ channel.

The tensor form factors T_2 and T_3 are related to T_1 as

$$T_2^{\text{Asymp. LO}}(z, s) = \frac{T_1^{\text{Asymp. LO}}(z, s)}{s}, \quad (10)$$

$$T_3^{\text{Asymp. LO}}(z, s) = T_1^{\text{Asymp. LO}}(z, s). \quad (11)$$

The higher order QCD and relativistic corrections for the vector and axial-vector form factors for B_c meson into a S-wave charmonium can be found in Refs. [14, 15, 17, 44]. We have confirmed all the previous results for the NLO corrections to the vector and axial-vector form factors. The relativistic corrections for the tensor form factors for $B_c \rightarrow J/\psi$ have been performed in Ref. [45]. In the following section we will study the NLO QCD corrections to the tensor form factors for both $B_c \rightarrow \eta_c$ and $B_c \rightarrow J/\psi$ channels. The precision predictions of various form factors shall improve the standard model theoretical uncertainty and determine the possible pattern of new physics in $R(\eta_c)$ and $R(J/\psi)$ observables.

III. QCD CORRECTION TO $B_c \rightarrow \eta_c, J/\psi$ TENSOR FORM FACTORS

We next calculate the NLO QCD corrections to the tensor form factors of $B_c \rightarrow (\eta_c, J/\psi)$ transitions. At LO, the form factors come from two tree diagrams in Fig. 1. At NLO, the form factors receive contributions from various 1-loop Feynman diagrams in Fig. 2. These 1-loop diagrams include the self-energy correction, vertex correction, box and pentagon correction.

On the calculation of the 1-loop diagrams, we adopt the Feynman gauge and use dimensional regularization to regularize the occurring UV and IR divergences. First, we apply the package FeynArts [46] to generate the corresponding Feynman diagrams and amplitudes. We implement the package FeynCalc [47] to handle amplitudes, i.e., contract indexes, simplify Dirac Gamma matrixes, and obtain traces. Then employing the package Apart [48] for partial fractions, the full 1-loop amplitudes, including the self-correction, vertex cor-

rection, box and pentagon correction are expressed as the linear combination of the standard Passarino-Veltman scalar integrals A0, B0, C0, D0¹. We use Package-X [50] to analytically calculate these Feynman integrals.

The 1-loop self-energy and vertex correction diagrams have the UV divergences, which are thought to be cancelled by the counter-term in standard high-order calculation procedure. But an additional renormalization factor Z_Γ for certain current is also required. The renormalization constants include Z_2 , Z_3 , Z_m , Z_g , and Z_Γ (see Ref. [44, 51]), referring to quark field, gluon field, quark mass, strong coupling constant g_s , and tensor current respectively. In our calculation the Z_3 , Z_g , Z_Γ are defined in the modified-minimal-subtraction ($\overline{\text{MS}}$) scheme, while for Z_2 and Z_m the on-shell (OS) scheme is employed, which tells

$$\delta Z_m = -3C_F \frac{\alpha_s}{4\pi} \left[\frac{1}{\epsilon_{UV}} + \ln \frac{\mu^2}{m^2} + \frac{4}{3} + O(\epsilon) \right] + O(\alpha_s^2), \quad (12)$$

$$\delta Z_2 = -C_F \frac{\alpha_s}{4\pi} \left[\frac{1}{\epsilon_{UV}} + \frac{2}{\epsilon_{IR}} + 3 \ln \frac{\mu^2}{m^2} + 4 + O(\epsilon) \right] + O(\alpha_s^2), \quad (13)$$

$$\delta Z_3 = \frac{\alpha_s}{4\pi} \left[(\beta_0 - 2C_A) \frac{1}{\epsilon_{UV}} + O(\epsilon) \right] + O(\alpha_s^2), \quad (14)$$

$$\delta Z_g = -\frac{\beta_0}{2} \frac{\alpha_s}{4\pi} \left[\frac{1}{\epsilon_{UV}} + O(\epsilon) \right] + O(\alpha_s^2), \quad (15)$$

$$\delta Z_\Gamma = C_F \frac{\alpha_s}{4\pi} \left[\frac{1}{\epsilon_{UV}} + O(\epsilon) \right] + O(\alpha_s^2). \quad (16)$$

Here, $\delta Z_i = Z_i - 1$. $\beta_0 = (11/3)C_A - (2/3)n_f$ is the one-loop coefficient of the QCD beta function, μ is the renormalization scale, and note that δZ_Γ will vanish for vector and axial-vector currents.

It is noted that these renormalization constants are involved in certain counter-term diagrams, but some of them may disappear in the final renormalization formulae since they will cancel by each other. Now we can write down the renormalization formula for the form factors. Take the $B_c \rightarrow \eta_c$ transition matrix element for example:

$$\begin{aligned} \langle \eta_c | \bar{c} \Gamma b | B_c \rangle &= (-ig_s)^2 \int \int d^4x d^4y \\ &\quad \langle \eta_c | T A^\mu(x) A^\nu(y) j_\mu(x) j_\nu(y) (\bar{c} \Gamma b)(0) | B_c \rangle \\ &= Z_g^2 (-ig_s^R)^2 \int \int d^4x d^4y \int \frac{d^4k}{(2\pi)^4} \frac{e^{-ik \cdot (x-y)}}{k^2 + i0} \\ &\quad Z_\Gamma Z_{2,c}^{3/2} Z_{2,b}^{1/2} \langle \eta_c | T j_\mu^R(x) j_\nu^R(y) (\bar{c} \Gamma b)^R(0) | B_c \rangle^R, \end{aligned} \quad (17)$$

where the renormalized matrix element has been labelled by a sub-letter R . The heavy quark mass which is not explicitly written out should be also renormalized. j_μ is the conserved

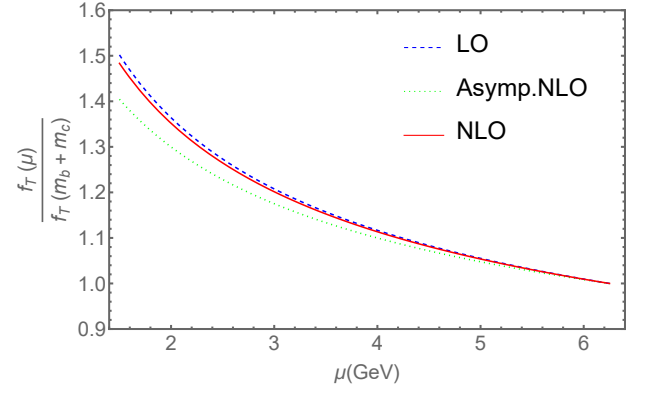


FIG. 3: The renormalization scale dependence of the form factor f_T at LO, asymptotic NLO and complete NLO. We set the form factors at the maximum recoil point, $q^2 = 0$. Herein μ runs from m_c to $m_b + m_c$ with fixed quark mass $m_c = 1.5\text{GeV}$ and $m_b = 4.75\text{GeV}$.

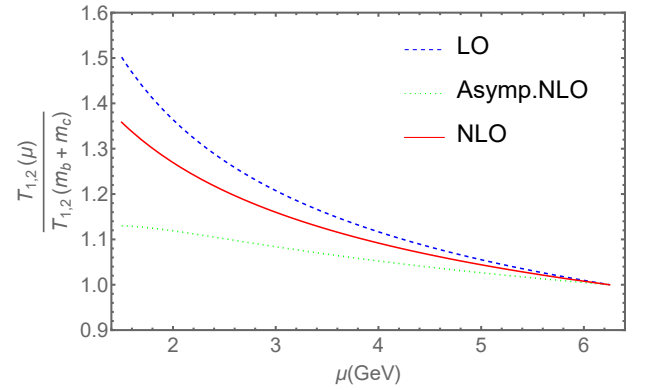


FIG. 4: The renormalization scale dependence of the form factors T_1 and T_2 at LO, asymptotic NLO and complete NLO. We set the form factors at the maximum recoil point, $q^2 = 0$, which leads to $T_1(q^2 = 0) = T_2(q^2 = 0)$. Herein μ runs from m_c to $m_b + m_c$ with fixed quark mass $m_c = 1.5\text{GeV}$ and $m_b = 4.75\text{GeV}$.

heavy quark vector current which does not need the renormalization, i.e. $j_\mu = j_\mu^R$ for conserved current. Similarly, $Z_\Gamma = 1$ for the flavor-changed vector and axial-vector current. While we have $Z_\Gamma = 1 + \delta Z_\Gamma \neq 1$ for the flavor-changed tensor current.

After summing up all of the contributions, we find both the UV and IR poles indeed cancel respectively, and obtain complete analytical finite results of the form factors. At last, we use Mathematica Function Series to obtain asymptotic expressions of the form factors in the hierarchy heavy quark limit. All of the analytical calculations have been numerically checked by the Package AMFlow [52] and Package FIESTA [53], which are consistent with each other.

The asymptotic expressions of form factors in the hierarchy heavy quark limit are presented in the Appendix. Note that the NLO QCD correction to $B_c \rightarrow \eta_c$ tensor form factor f_T has been investigated in Ref. [44]. We have confirmed their results of the form factors in the paper [44]. In addition, we also obtained the NLO QCD correction to $B_c \rightarrow J/\psi$ ten-

¹ However, the five-point integrals in the sub-diagram (18) in Fig. 2, can only be reduced to A0, B0, C0, D0 by integration by Parts (IBP) [49] without setting scaleless integrals to zero to distinguish UV and IR divergences.

form factors $T_{1,2,3}$, which are important input to precisely study the $R(J/\psi)$ anomaly [54]. The method may also apply in the transition of double heavy diquark system [55].

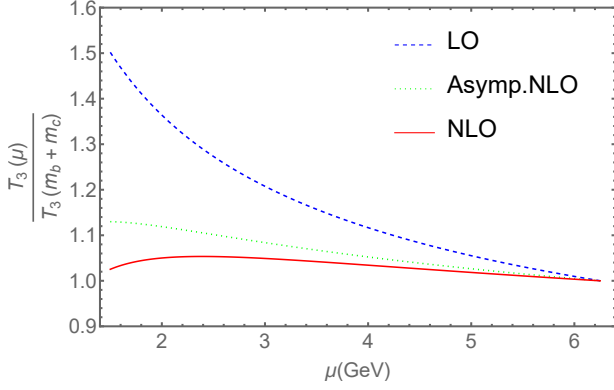


FIG. 5: The renormalization scale dependence of the form factors T_3 at LO, asymptotic NLO and complete NLO. We set the form factors at the maximum recoil point, $q^2 = 0$. Herein μ runs from m_c to $m_b + m_c$ with fixed quark mass $m_c = 1.5\text{GeV}$ and $m_b = 4.75\text{GeV}$.

IV. NUMERICAL RESULTS AND DISCUSSIONS

In the following numerical calculation, the one loop result for strong coupling constant is used, i.e.

$$\alpha_s(\mu) = \frac{4\pi}{(\frac{11}{3}C_A - \frac{2}{3}n_f)\ln(\frac{\mu^2}{\Lambda_{QCD}^2})}, \quad (18)$$

where the typical QCD scale Λ_{QCD} is related to n_f . For example $\Lambda_{QCD}^{n_f=5} = 87\text{MeV}$ is determined by $\alpha_s(m_Z) = 0.1179$ with $m_Z = 91.1876\text{GeV}$. Λ_{QCD} will increase if one use the high-order result for strong coupling constant, however, it is not necessary and only required if we also take the high-order corrections to the form factors. Because we have treated the B_c meson and the S-wave charmonium as nonrelativistic bound states, the pole mass of heavy flavor quarks is adopted as: $m_b = 4.75 \pm 0.05\text{GeV}$ and $m_c = 1.5 \pm 0.05\text{GeV}$.

First we investigate the renormalization scale dependence of the form factors. To eliminate the uncertainty of nonperturbative NRQCD LDMEs, we define $f_T(\mu)/f_T(m_b + m_c)$ and $T_i(\mu)/T_i(m_b + m_c)$ which are independent on the nonperturbative NRQCD LDMEs. We then plot the renormalization scale dependence of tensor form factors at the LO, asymptotic NLO and complete NLO results in Figs. 3, 4, and 5. In general, the scale dependence at NLO is obviously depressed relative to the LO case. Naming, the $\beta_0\alpha_s^2\ln(\mu^2)$ terms in the form factors are cancelled by the scale dependence in the strong coupling constant. But an additional renormalization constant Z_Γ is introduced for tensor form factors and it leads to a scale dependent term proportional to $C_F\alpha_s^2\ln(\mu^2)$ which can not be cancelled. Thus it is reasonable that the scale dependence of tensor form factor f_T at NLO is still large.

Next we will focus on the theoretical predictions of tensor form factors in B_c to a S-wave charmonium. To avoid

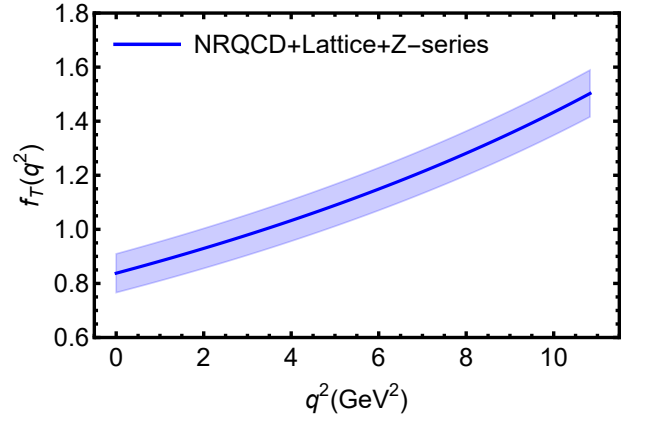


FIG. 6: The full curve of physical tensor form factor $f_T(q^2)$ for $B_c \rightarrow \eta_c$ transition with $0 \leq q^2 \leq (m_{B_c} - m_{\eta_c})^2$. The blue curve with error band is the result of our polynomial fit in z-series combined with NRQCD calculation and the HPQCD lattice data of vector form factors for $B_c \rightarrow \eta_c$ [9].

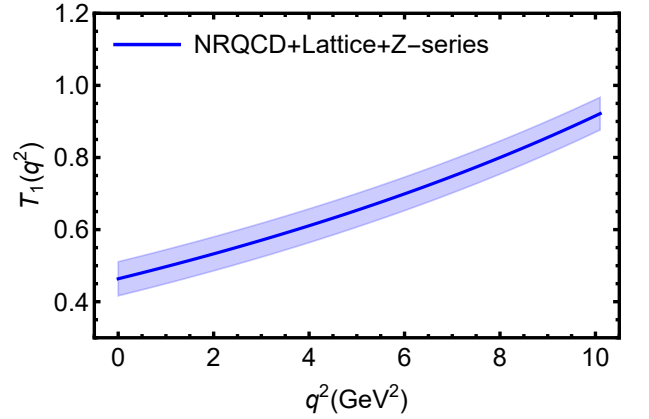


FIG. 7: The full curve of physical tensor form factor $T_1(q^2)$ for $B_c \rightarrow J/\psi$ transition with $0 \leq q^2 \leq (m_{B_c} - m_{J/\psi})^2$. The blue curve with error band is the result of our polynomial fit in z-series combined with NRQCD calculation and the HPQCD lattice data of vector and axial-vector form factors for $B_c \rightarrow J/\psi$ [10].

the uncertainties from NRQCD LDMEs, we can employ the HPQCD lattice data of vector and axial-vector form factors in B_c to a S-wave charmonium [9, 10]. Combined the analytical expressions of vector, axial-vector and tensor factors in NRQCD framework, we can furthermore obtain the tensor form factors.

However, the perturbative calculation in NRQCD is valid when the transferred momentum is large. Thus the analytical expressions of vector, axial-vector and tensor factors in NRQCD framework are not applicable for minimum momentum recoil region. Thus we will use the Z-series method [56–59] to do the extrapolation. The tensor form factors can be rewritten as [60, 61]

$$F_i(t) = \frac{1}{1 - t/m_R^2} \sum_{k=0}^{\infty} \alpha_k^i z^k(t, t_0), \quad (19)$$

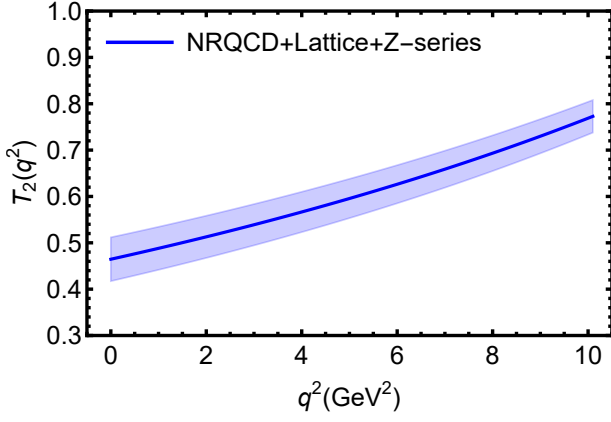


FIG. 8: The same as Fig. 7, but for the physical tensor form factor $T_2(q^2)$ for $B_c \rightarrow J/\psi$.

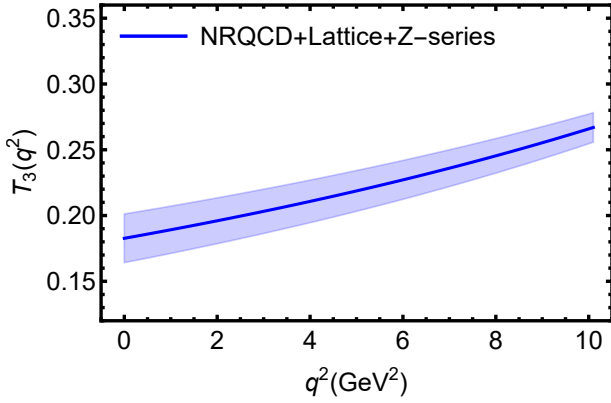


FIG. 9: The same as Fig. 7, but for the physical tensor form factor $T_3(q^2)$ for $B_c \rightarrow J/\psi$.

with

$$z = \frac{\sqrt{t_+ - t} - \sqrt{t_+ - t_0}}{\sqrt{t_+ - t} + \sqrt{t_+ - t_0}}, \quad (20)$$

$$t_0 = t_+ \left(1 - \sqrt{1 - \frac{t_-}{t_+}} \right), \quad (21)$$

$$t_{\pm} = \left(m_{B_c} \pm m_{\eta_c(J/\psi)} \right)^2, \quad (22)$$

where $t = q^2$. m_R are the masses of the low-lying B_c resonance. Here the series of parameter z can be truncated to 2nd order because $z(q^2) \sim 0.02$ in B_c to a S-wave charmonium [62].

We plot the full curve of physical tensor form factors f_T and $T_{1,2,3}$ for B_c to a S-wave charmonium in Figs. 6, 7, 8,

and 9. Our results of $B_c \rightarrow \eta_c$ and $B_c \rightarrow J/\psi$ tensor form factors at maximum recoil $q^2 = 0$ are listed in Tab. I, together with the results from other literatures. The uncertainties of our numerical results in Tab. I are from the HPQCD lattice data uncertainties of vector and axial-vector form factors [9, 10].

TABLE I: Tensor form factors at maximum momentum recoil point $q^2 = 0$ calculated in this paper and other literatures.

	$f_T(0)$	$T_1(0) = T_2(0)$	$T_3(0)$
NRQCD+Lattice	0.85 ± 0.07	0.46 ± 0.05	0.18 ± 0.02
CCQM[63]	0.93	0.56	0.20
CLFQM(type-II)[64]	$0.90^{+0.17}_{-0.22}$	$0.56^{+0.16}_{-0.17}$	$0.19^{+0.03}_{-0.03}$
QCDSR[60]	0.93 ± 0.07	0.47 ± 0.04	0.19 ± 0.01

V. CONCLUSION

While the lattice QCD have performed a state-of-the-art work on the vector and axial-vector form factors for B_c meson into a S-wave charmonium, analyzing the pattern of new physics in $R(\eta_c)$ and $R(J/\psi)$ require more theoretical inputs. In this paper, we calculated the analytical NLO corrections to tensor form factors for the transitions of B_c meson into a S-wave charmonium, the η_c and J/ψ . The compact asymptotic expression of tensor form factors in heavy bottom quark limit are presented. Combined the strict NLO results for vector, axial-vector, and tensor form factors and the HPQCD lattice data of vector and axial-vector form factors, we obtained the full curve of the physical tensor form factors $f_T(q^2)$ and $T_{1,2,3}(q^2)$ for the considered $B_c \rightarrow \eta_c, J/\psi$ charmonia. These results are useful to precisely study the semileptonic decays of B_c meson into a S-wave charmonium such as the $R(J/\psi)$ anomaly.

Acknowledgements

This work is supported by NSFC under Grant No. 11775117 and No. 12075124, and by Natural Science Foundation of Jiangsu under Grant No. BK20211267.

Appendix

In this appendix, we have listed the analytical expression of tensor form factors for B_c meson into a S-wave charmonium in the hierarchy heavy quark limit, i.e. $m_b \rightarrow \infty$, $m_c \rightarrow \infty$, and $z = m_c/m_b \rightarrow 0$. In general, we have $z = m_c/m_b$ and $s = 1/(1 - q^2/m_b^2)$. For $B_c \rightarrow \eta_c$ transition we have

$$\begin{aligned}
\frac{f_T^{\text{NLO}}(z, s)}{f_T^{\text{LO}}(z, s)} = & 1 + \frac{\alpha_s}{4\pi} \left\{ \left(\frac{11C_A}{3} - \frac{2n_f}{3} \right) \ln \frac{2\mu^2 s}{zm_b^2} - \frac{10n_f}{9} - \frac{\ln z}{2} - \frac{\ln s}{2} - 2 \ln 2 + \frac{\pi^2}{6} \right. \\
& + C_A \left[-\frac{\ln^2 z}{4} + \left(-\frac{\ln s}{2} - \frac{3 \ln 2}{2} - \frac{1}{2} \right) \ln z + \left(\frac{1}{2} - 2s \right) \text{Li}_2(1-2s) + \left(s - \frac{1}{2} \right) \text{Li}_2(1-s) \right. \\
& + \frac{1}{4} (-2s-1) \ln^2 s + \left((-2s-1) \ln 2 + \frac{s}{1-2s} \right) \ln s + \left(-s - \frac{1}{2} \right) \ln^2 2 + \frac{(1-3s) \ln 2}{2s-1} - \frac{1}{12} \pi^2 (2s+1) + \frac{67}{9} \Big] \\
& + C_F \left[-\ln \frac{\mu^2}{m_b^2} + \frac{5 \log^2 z}{4} + \left(\frac{5 \ln s}{2} + 6 \ln 2 - \frac{23}{4} \right) \ln z + (4s-1) \text{Li}_2(1-2s) + (3-2s) \text{Li}_2(1-s) \right. \\
& + \left(s + \frac{9}{4} \right) \ln^2 s + \left((4s+5) \ln 2 + \frac{s(4(34-11s)s-101)+23}{4(1-2s)^2(s-1)} \right) \ln s + \left(2s + \frac{5}{2} \right) \ln^2 2 \\
& + \left. \left. \frac{(4s(6s-7)+7) \ln 2}{2(1-2s)^2} + \frac{1}{12} \left(\pi^2 (4s+19) + \frac{6}{2s-1} - 207 \right) \right] \right\}, \tag{23}
\end{aligned}$$

and at maximum recoil point ($s = 1$ or $q^2 = 0$)

$$\begin{aligned}
\frac{f_T^{\text{NLO}}(z, 1)}{f_T^{\text{LO}}(z, 1)} = & 1 + \frac{\alpha_s}{4\pi} \left\{ \left(\frac{11C_A}{3} - \frac{2n_f}{3} \right) \ln \frac{2\mu^2}{zm_b^2} - \frac{10n_f}{9} - \frac{\ln z}{2} - 2 \ln 2 + \frac{\pi^2}{6} \right. \\
& + C_A \left[-\frac{1}{4} \ln^2 z + \left(-\frac{3 \ln 2}{2} - \frac{1}{2} \right) \ln z - \frac{3 \ln^2 2}{2} - 2 \ln 2 - \frac{\pi^2}{8} + \frac{67}{9} \right] \\
& + C_F \left[-\ln \frac{\mu^2}{m_b^2} + \frac{5 \ln^2 z}{4} + \left(6 \ln 2 - \frac{23}{4} \right) \ln z + \frac{9 \ln^2 2}{2} + \frac{3 \ln 2}{2} + \frac{5\pi^2}{3} - \frac{53}{4} \right] \Big\}. \tag{24}
\end{aligned}$$

Note that the above NLO result of $B_c \rightarrow \eta_c$ tensor form factor f_T is in agreement with the previous calculation in Ref. [44].

For $B_c \rightarrow J/\psi$ transition we have

$$\begin{aligned}
\frac{T_1^{\text{NLO}}(z, s)}{T_1^{\text{LO}}(z, s)} = & 1 + \frac{\alpha_s}{4\pi} \left\{ \left(\frac{11C_A}{3} - \frac{2n_f}{3} \right) \ln \frac{2\mu^2 s}{zm_b^2} - \frac{10n_f}{9} \right. \\
& + C_A \left[-\frac{2s \ln^2 z}{4s+1} + \left(\left(\frac{1}{4s+1} - 1 \right) \ln s + \left(\frac{6}{4s+1} - 2 \right) \ln 2 - \frac{6s}{4s+1} \right) \ln z \right. \\
& + \frac{(6s-4) \text{Li}_2(1-2s)}{4s+1} + \left(\frac{5}{4s+1} - 1 \right) \text{Li}_2(1-s) - \frac{s \ln^2 s}{4s+1} + \left(-\frac{2s \ln 2}{4s+1} - \frac{6s}{4s+1} \right) \ln s \\
& - \frac{5s \ln^2 2}{4s+1} - \frac{6s \ln 2}{4s+1} + \frac{268s - 3\pi^2(3s+2) + 85}{36s+9} \Big] \\
& + C_F \left[-\ln \frac{\mu^2}{m_b^2} + \left(1 - \frac{2}{4s+1} \right) \ln^2 z + \left(\left(2 - \frac{4}{4s+1} \right) \ln s + \left(10 - \frac{12}{4s+1} \right) \ln 2 + \frac{1}{-4s-1} - 5 \right) \ln z \right. \\
& + \left(\frac{9}{4s+1} - 3 \right) \text{Li}_2(1-2s) + \left(4 - \frac{8}{4s+1} \right) \text{Li}_2(1-s) + \left(\left(7 - \frac{3}{4s+1} \right) \ln 2 - \frac{5}{4s+1} - 2 \right) \ln s \\
& + \frac{6s \ln^2 s}{4s+1} + \frac{(22s+2) \ln^2 2}{4s+1} + \left(9 - \frac{8}{4s+1} \right) \ln 2 + \frac{\pi^2(2s-1)}{12s+3} - 17 \Big] \Big\}, \tag{25}
\end{aligned}$$

$$\frac{T_1^{\text{NLO}}(z, s)}{T_1^{\text{LO}}(z, s)} = \frac{T_2^{\text{NLO}}(z, s)}{T_2^{\text{LO}}(z, s)} = \frac{T_3^{\text{NLO}}(z, s)}{T_3^{\text{LO}}(z, s)}. \tag{26}$$

and at maximum recoil point ($s = 1$ or $q^2 = 0$)

$$\begin{aligned} \frac{T_1^{\text{NLO}}(z, 1)}{T_1^{\text{LO}}(z, 1)} = & 1 + \frac{\alpha_s}{4\pi} \left\{ \left(\frac{11C_A}{3} - \frac{2n_f}{3} \right) \ln \frac{2\mu^2}{zm_b^2} - \frac{10n_f}{9} \right. \\ & + C_A \left[-\frac{2}{5} \ln^2 z + \left(-\frac{4 \ln 2}{5} - \frac{6}{5} \right) \ln z - \ln^2 2 - \frac{6 \ln 2}{5} + \frac{1}{90} (706 - 33\pi^2) \right] \\ & \left. + C_F \left[-\ln \frac{\mu^2}{m_b^2} + \frac{3 \ln^2 z}{5} + \left(\frac{38 \ln 2}{5} - \frac{26}{5} \right) \ln z + \frac{24 \ln^2 2}{5} + \frac{37 \ln 2}{5} + \frac{\pi^2}{6} - 17 \right] \right\}, \end{aligned} \quad (27)$$

$$\frac{T_1^{\text{NLO}}(z, 1)}{T_1^{\text{LO}}(z, 1)} = \frac{T_2^{\text{NLO}}(z, 1)}{T_2^{\text{LO}}(z, 1)} = \frac{T_3^{\text{NLO}}(z, 1)}{T_3^{\text{LO}}(z, 1)}. \quad (28)$$

-
- [1] J. P. Lees *et al.* [BaBar], Phys. Rev. Lett. **109**, 101802 (2012)
- [2] S. Hirose *et al.* [Belle], Phys. Rev. Lett. **118**, no.21, 211801 (2017)
- [3] R. Aaij *et al.* [LHCb], Phys. Rev. D **97**, 072013 (2018)
- [4] R. Aaij *et al.* [LHCb], Phys. Rev. Lett. **120**, no.12, 121801 (2018)
- [5] F. U. Bernlochner, M. F. Sevilla, D. J. Robinson and G. Wormser, Rev. Mod. Phys. **94**, 015003 (2022)
- [6] J. Harrison *et al.* [LATTICE-HPQCD], Phys. Rev. Lett. **125**, 222003 (2020)
- [7] K. Cheung, Z. R. Huang, H. D. Li, C. D. Lü, Y. N. Mao and R. Y. Tang, Nucl. Phys. B **965**, 115354 (2021)
- [8] Z. R. Huang, Y. Li, C. D. Lu, M. A. Paracha and C. Wang, Phys. Rev. D **98**, 095018 (2018)
- [9] B. Colquhoun *et al.* [HPQCD], PoS **LATTICE2016**, 281 (2016)
- [10] J. Harrison *et al.* [HPQCD], Phys. Rev. D **102**, 094518 (2020)
- [11] C. H. Chang and Y. Q. Chen, Phys. Rev. D **49**, 3399-3411 (1994)
- [12] V. V. Kiselev, O. N. Pakhomova and V. A. Saleev, J. Phys. G **28**, 595-606 (2002)
- [13] G. Bell and T. Feldmann, Nucl. Phys. B Proc. Suppl. **164**, 189-192 (2007)
- [14] C. F. Qiao, P. Sun, F. Yuan, JHEP **08**, 087 (2012)
- [15] C. F. Qiao and R. L. Zhu, Phys. Rev. D **87**, 014009 (2013)
- [16] C. F. Qiao, P. Sun, D. Yang and R. L. Zhu, Phys. Rev. D **89**, 034008 (2014)
- [17] R. Zhu, Y. Ma, X. L. Han and Z. J. Xiao, Phys. Rev. D **95**, 094012 (2017)
- [18] R. Zhu, Nucl. Phys. B **931**, 359-382 (2018)
- [19] D. s. Du and Z. Wang, Phys. Rev. D **39**, 1342 (1989)
- [20] J. F. Sun, D. S. Du and Y. L. Yang, Eur. Phys. J. C **60**, 107-117 (2009)
- [21] W. F. Wang, Y. Y. Fan and Z. J. Xiao, Chin. Phys. C **37**, 093102 (2013)
- [22] Z. Rui and Z. T. Zou, Phys. Rev. D **90**, 114030 (2014)
- [23] X. Liu, H. n. Li and Z. J. Xiao, Phys. Lett. B **811**, 135892 (2020)
- [24] J. M. Shen, X. G. Wu, H. H. Ma and S. Q. Wang, Phys. Rev. D **90**, 034025 (2014)
- [25] P. Colangelo, G. Nardulli and N. Paver, Z. Phys. C **57**, 43-50 (1993)
- [26] V. V. Kiselev, A. K. Likhoded and A. I. Onishchenko, Nucl. Phys. B **569**, 473-504 (2000)
- [27] K. Azizi, H. Sundu and M. Bayar, Phys. Rev. D **79**, 116001 (2009)
- [28] T. Huang and F. Zuo, Eur. Phys. J. C **51**, 833-839 (2007)
- [29] W. Wang, Y. L. Shen and C. D. Lu, Phys. Rev. D **79**, 054012 (2009)
- [30] H. W. Ke, T. Liu and X. Q. Li, Phys. Rev. D **89**, 017501 (2014)
- [31] M. A. Nobes and R. M. Woloshyn, J. Phys. G **26**, 1079-1094 (2000)
- [32] D. Ebert, R. N. Faustov and V. O. Galkin, Phys. Rev. D **68**, 094020 (2003)
- [33] M. A. Ivanov, J. G. Korner and P. Santorelli, Phys. Rev. D **71**, 094006 (2005) [erratum: Phys. Rev. D **75**, 019901 (2007)]
- [34] D. Ebert, R. N. Faustov and V. O. Galkin, Phys. Rev. D **82**, 034019 (2010)
- [35] L. Nayak, P. C. Dash, S. Kar and N. Barik, [arXiv:2204.04453 [hep-ph]].
- [36] E. Hernandez, J. Nieves and J. M. Verde-Velasco, Phys. Rev. D **74**, 074008 (2006)
- [37] R. Zhu, X. L. Han, Y. Ma and Z. J. Xiao, Eur. Phys. J. C **78**, 740 (2018)
- [38] X. G. He, W. Wang and R. L. Zhu, J. Phys. G **44**, 014003 (2017)
- [39] G. T. Bodwin, E. Braaten and G. P. Lepage, Phys. Rev. D **51**, 1125-1171 (1995) [erratum: Phys. Rev. D **55**, 5853 (1997)]
- [40] N. Isgur and M. B. Wise, Phys. Rev. D **42**, 2388-2391 (1990)
- [41] P. Ball and V. M. Braun, Phys. Rev. D **58**, 094016 (1998)
- [42] A. Ali, P. Ball, L. T. Handoko and G. Hiller, Phys. Rev. D **61**, 074024 (2000)
- [43] M. Beneke and T. Feldmann, Nucl. Phys. B **592**, 3-34 (2001)
- [44] G. Bell, Ph.D. Thesis, [arXiv:0705.3133 [hep-ph]].
- [45] D. Shen, H. Ren, F. Wu and R. Zhu, Int. J. Mod. Phys. A **36**, 2150135 (2021)
- [46] T. Hahn, Comput. Phys. Commun. **140**, 418-431 (2001)
- [47] V. Shtabovenko, R. Mertig and F. Orellana, Comput. Phys. Commun. **256**, 107478 (2020)
- [48] F. Feng, Comput. Phys. Commun. **183**, 2158-2164 (2012)
- [49] K. G. Chetyrkin and F. V. Tkachov, Nucl. Phys. B **192**, 159-204 (1981)
- [50] H. H. Patel, Comput. Phys. Commun. **218**, 66-70 (2017)
- [51] C. W. Bauer, S. Fleming, D. Pirjol and I. W. Stewart, Phys. Rev. D **63**, 114020 (2001)
- [52] X. Liu and Y. Q. Ma, [arXiv:2201.11669 [hep-ph]].

- [53] A. V. Smirnov, N. D. Shapurov and L. I. Vysotsky, [arXiv:2110.11660 [hep-ph]].
- [54] R. Y. Tang, Z. R. Huang, C. D. Lü and R. Zhu, [arXiv:2204.04357 [hep-ph]].
- [55] Q. Qin, Y. J. Shi, W. Wang, G. H. Yang, F. S. Yu and R. Zhu, Phys. Rev. D **105**, L031902 (2022)
- [56] C. G. Boyd, B. Grinstein and R. F. Lebed, Phys. Rev. D **56**, 6895-6911 (1997)
- [57] I. Caprini, L. Lellouch and M. Neubert, Nucl. Phys. B **530**, 153-181 (1998)
- [58] C. Bourrely, I. Caprini and L. Lellouch, Phys. Rev. D **79**, 013008 (2009) [erratum: Phys. Rev. D **82**, 099902 (2010)]
- [59] A. Bharucha, T. Feldmann and M. Wick, JHEP **09**, 090 (2010)
- [60] D. Leljak, B. Melic and M. Patra, JHEP **05**, 094 (2019)
- [61] X. Q. Hu, S. P. Jin and Z. J. Xiao, Chin. Phys. C **44**, 023104 (2020)
- [62] W. Wang and R. Zhu, Int. J. Mod. Phys. A **34**, 1950195 (2019)
- [63] C. T. Tran, M. A. Ivanov, J. G. Körner and P. Santorelli, Phys. Rev. D **97**, 054014 (2018)
- [64] Q. Chang, X. L. Wang and L. T. Wang, Chin. Phys. C **44**, no.8, 083105 (2020)